Computational Materials Science 77 (2013) 343–347

Contents lists available at SciVerse ScienceDirect

Computational Materials Science

journal homepage: www.elsevier.com/locate/commatsci

Dependence of Peierls stress on lattice strains in silicon

Z. Li, N. Mathew, R.C. Picu *

Department of Mechanical, Aerospace and Nuclear Engineering, Rensselaer Polytechnic Institute, Troy, NY 12180, United States

ARTICLE INFO

Article history:
Received 4 March 2013
Received in revised form 17 April 2013
Accepted 29 April 2013
Available online 30 May 2013

Keywords:
Dislocations
Lattice instabilities
Peierls stress

ABSTRACT

Several non-Schmid effects of plasticity in Si are discussed in this article. The contribution of shear strain applied in the direction of the Burgers vector and normal to it in the glide plane, and of strain applied normal to the glide plane to defining the Peierls stress are analyzed. The analysis is performed using a combination of atomistic simulations and the Peierls–Nabarro model based on generalized stacking faults. It is shown that a shear strain acting in the direction of the Burgers vector decreases the Peierls stress and the effect is due to the reduction of the shear modulus. Bonding across the glide plane has the most important contribution to the Peierls stress, but the elastic non-linearity of the surrounding material contributes to reducing the instability threshold. A shear strain acting perpendicular to the Burgers vector has no effect on the Peierls stress. A compressive strain normal to the glide plane reduces the Peierls stress for shuffle dislocations and has a weak increasing effect on the critical stress of glide-set dislocations.

1. Introduction

Plastic deformation in crystalline materials takes place by the motion of dislocations on specific slip systems. The resistance dislocations face during motion is due to their interaction with the lattice and with other obstacles such as forest dislocations, solute atoms, precipitates, grain and twin boundaries. At low temperatures and in materials with strong bonding, the dominant contribution comes from the Peierls stress required to move an isolated dislocation in the perfect lattice.

Silicon has a diamond cubic lattice with strong bonding and undergoes a brittle-to-ductile transition at approximately 873 °K [1]. In this material, dislocations are strongly pinned by the Peierls barriers. The magnitude of the critical stress has been studied extensively experimentally [2,3], theoretically [4–6] and using atomistic simulations [7,8]. The main slip system is $\{111\}\langle 110\rangle$. There are two types of glide planes denoted by shuffle and glide, with the shuffle planes having an interplanar distance of 2.35 Å, and the glide planes being spaced 0.78 Å apart. A simple geometric model suggests that the density of bonds crossing the shuffle plane is smaller than that for the glide plane. It is currently accepted that the activity in the shuffle plane dominates at low temperatures and high resolved shear stresses, while at high temperatures motion in the glide system controls plasticity. As confirmed by ab initio and atomistic models, glide dislocations are dissociated in partials, while shuffle dislocations are not. This helps identifying the nature of slip in electron microscopy, as the simple observation of a compact, undissociated core indicates that the respective dislocation resides in the shuffle plane.

The interplanar potential is usually characterized by the γ-surface. The standard γ-surface is computed by separating the crystal in two parts across a glide plane and evaluating the variation of the energy per unit area associated with the relative shift of the two blocks in the selected plane. Hence, the γ-surface has minima at shifts equal to the lattice periodicity. Additional minima appear for certain configurations which correspond to stacking faults. In Si, no minimum is observed in the shuffle plane, while the glide plane γ-surface has a minimum at a relative shift of 1/6 $\langle 112\rangle$, which corresponds to the Burgers vector of a partial dislocation. The minimum energy paths on the γ-surface linking these minima indicate the preferred glide mode of the crystal and define the structure and evolution of the core of dislocations moving over the Peierls barriers. The γ-surface in Si was computed for both planes using ab initio [9] and atomistic [10] simulations.

The Peierls stress can be computed directly from atomistic simulations, by effectively forcing a dislocation to move under an applied far-field. The Peierls stress is usually computed in situations in which dislocations remain straight during motion, despite the fact that in lattices with high resistance dislocations move by the kink mechanism [11]. The critical stress is also estimated using the Peierls–Nabarro model (PN). In this semi-analytical formulation the core is represented as a continuous distribution of infinitesimal dislocations on the glide plane. The core structure is described by a distribution of infinitesimal dislocation density (slip magnitude). The solution results by requiring that the distribution is in equilibrium under the action of the mutual repulsion of the infinitesimal dislocations and the lattice rebound forces. An

* Corresponding author. Tel.: +1 518 276 2195.
E-mail address: picuc@rpi.edu (R.C. Picu).

0927-0256/$ - see front matter © 2013 Elsevier B.V. All rights reserved.
http://dx.doi.org/10.1016/j.commatsci.2013.04.068

additional term appears when a resolved shear stress is applied. Under the action of this perturbation, the core distorts. The Peierls stress is evaluated as the applied stress for which no solution can be found.

In the initial literature on the subject, the rebound force was computed from the interplanar potential which was assumed to be sinusoidal [12]. An analytic solution can be obtained in this case. In later refinements, the rebound force was computed as the derivative of the γ-surface [6].

Let us return now to the central problem discussed in this article and consider an isolated, straight dislocation in an infinite crystal. When the Peierls stress is evaluated in atomistic simulations, a shear strain is applied in the direction of the Burgers vector until instability is reached and the dislocation core shifts forward by at least one inter-atomic distance. At the instability, the surrounding lattice is elastically distorted and hence the local bonding is different from that in the unloaded lattice. Nevertheless, when the Peierls stress is evaluated using the PN model and the atomistically-determined γ-surface, the interplanar potential is computed by shifting the two blocks of atoms relative to each other as rigid entities. Hence, this γ-surface includes only the contribution from the distortion of bonds in the glide plane. It is therefore more natural to consider a γ-surface in which the two blocks are allowed to deform elastically in response to the applied stress, with the relative shift being applied simultaneously. This generalized γ-surface (GGS) was used recently in the context of dislocation nucleation [13].

One may question the need to use the PN model when predicting the Peierls stress in situations in which atomistic simulations are feasible. However, atomistic models provide simply a number: the value of the critical stress. The PN model, although an approximation, provides more insight into the physics that determines the lattice resistance to dislocation motion. Specifically, one identifies the contribution of the bonds across the glide plane (when the classical γ-surface is used), that of the bond distortion elsewhere in the model (when the GGS is used), and the effect of the non-linearity of the elastic material behavior.

The present study outlines these contributions to the Peierls stress. Three strains are considered: two shear strains acting in the glide plane, one along and one perpendicular to the Burgers vector, and a normal strain acting in the direction of the glide plane normal. The model and procedures used are described in Section 2, the results are discussed in Section 3 and conclusions are presented in closure.

2. Model and simulation procedures

Silicon is represented with the three-body Stillinger–Weber (SW) potential which has been used extensively in atomistic simulations [14]. A large number of potentials have been developed for Si, the most broadly used being SW, Tersoff [15,16] and EDIP [17]. Each of these potentials has strengths and weaknesses. Godet et al. [18] compared the three potentials against ab initio data (density functional theory-local density approximation, DFT–LDA) specifically with respect to their performance with respect to large shear strains applied in the shuffle and glide {1 1 1} planes. They conclude that the SW potential better reproduces the ab initio results with respect to the smoothness and the amplitude of the energy variation, and the localization of shear in the shuffle set. The SW potential provides the best approximation of the maximum restoring force for the $\langle 1\,1\,0\rangle$ direction in the shuffle plane and the $\langle 1\,1\,2\rangle$ direction in the glide plane, and for the theoretical shear strength and the strain associated with this critical stress in both planes. The un-relaxed unstable stacking fault energy for traces in the Burgers vector direction is best predicted for the $\langle 1\,1\,0\rangle$ direction in the shuffle plane by the SW potential, and for the $\langle 1\,1\,2\rangle$ direction of the glide plane by the EDIP potential. The values of the relaxed unstable stacking fault energy are best predicted by the Tersoff potential in both these crystal directions. Based on these findings, we conclude that the SW potential is best suited to represent the phenomena discussed in this article.

Atomistic models are used to determine the γ-surface under specific applied strain states. The three far fields considered in this work are shown schematically in Fig. 1. Vector s defines the interplanar shift in the glide plane and is always taken in the direction of the Burgers vector: $s \parallel b$, $|s|/|b| \in [0, 1]$. The far field strain, ε, loads the entire model, except the two atomic planes defining the glide plane, where the relative shift is entirely defined by s. If $\varepsilon = 0$, one recovers the configuration customarily used to evaluate the γ-surface (Fig. 1a); this situation is denoted as Case 1. Three other cases are considered: $v = \varepsilon \cdot n \parallel s \parallel b$ (Fig. 1b, Case 2), where the strain has exclusively a shear component in the glide plane and in the direction of the Burgers vector (n is the normal to the glide plane), $v = \varepsilon \cdot n \perp b$ (Fig. 1c, Case 3), where the strain has a shear component in the glide plane and in the direction perpendicular to the Burgers vector, and $v = \varepsilon \cdot n \parallel n$ (Fig. 1d, Case 4), where the strain has only a component perpendicular to the glide plane. These are the three elementary distortion modes that can be applied relative to the glide plane and b.

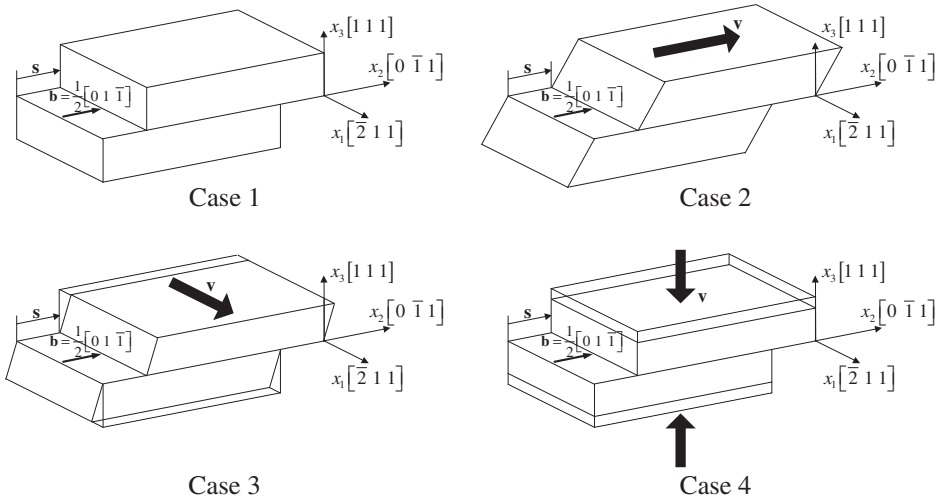

Fig. 1. Schematic representation of the loading conditions considered in this work.

The 3D simulation box has dimensions of $66 \times 61 \times 75$ Å^3, and contains 15,360 atoms. The crystal orientation is indicated in Fig. 1, with the relative shift being applied across a {1 1 1} plane. Periodic boundary conditions are used in x_1 and x_2 directions. The desired shift and far fields are imposed by affinely displacing all atoms.

We compute the traces of the γ-surface for all these loading cases and use them to evaluate the rebound force in the PN model. For completeness, it is useful to review the basic ideas of the PN model.

The core of the dislocation is represented by a distribution of infinitesimal dislocations whose density ρ defines the "shape" of the actual core and can be related to Δu, the displacement jump across the glide plane, by $\rho = \partial \Delta u(x)/\partial x$. The equilibrium condition of the distribution of infinitesimal dislocations requires the balance of the external stress field, the stress field produced by the infinitesimal dislocations, as well as the restoring stress due to lattice mismatch. Note that only the shear stress, τ, resolved in the glide plane and in the direction of b enters the equilibrium equation, which reads:

$$\tau + \frac{G}{2\pi(1-\nu)} \int_{-\infty}^{\infty} \frac{\rho(\zeta)d\zeta}{x-\zeta} - \left.\frac{\partial \gamma(\Delta u, \tau)}{\partial \Delta u}\right|_x = 0 \qquad (1)$$

The second term represents the stress field produced in the glide plane by the distribution of infinitesimal dislocations, with G being the corresponding shear modulus, and the third term is the restoring stress computed from the γ-surface. If the γ-surface is independent of the applied stress, one recovers Case 1. When the GGS is used instead (Cases 2 and 3), γ changes with τ. To calculate the Peierls stress, the applied stress is increased gradually while seeking a numerical solution for Eq. (1) at each step. The value of τ at which no solution can be found is considered the Peierls stress. When the GGS is used, multiple γ-surfaces, corresponding to various τ values are employed and the third term in Eq. (1) is evaluated by interpolation between these, as τ increases.

The value of the shear modulus, G, used in Eq. (1) deserves a comment. Fig. 2 shows the Si lattice in the {1 1 0} projection. Due to the different bonding across the glide and shuffle planes, the local, effective shear modulus as well as the local shear strains in the two planes are different. If deformation is linear elastic, one has $\tau = G\gamma$, $\tau = G_s\gamma_s$ and $\tau = G_g\gamma_g$, where the two indices indicate the shuffle and glide planes respectively. The moduli are related through the relation: $\frac{d_s+d_g}{G} = \frac{d_s}{G_s} + \frac{d_g}{G_g}$. From simulations we obtain a large difference between G_s and G_d. In both the direction of the full dislocation, $\langle 1\,1\,0\rangle$, and in the partial Burgers vector direction, $\langle 1\,1\,2\rangle$, one has $G_s = 36.2$ GPa, $G_d = 117$ GPa and $G = 43.6$ GPa.

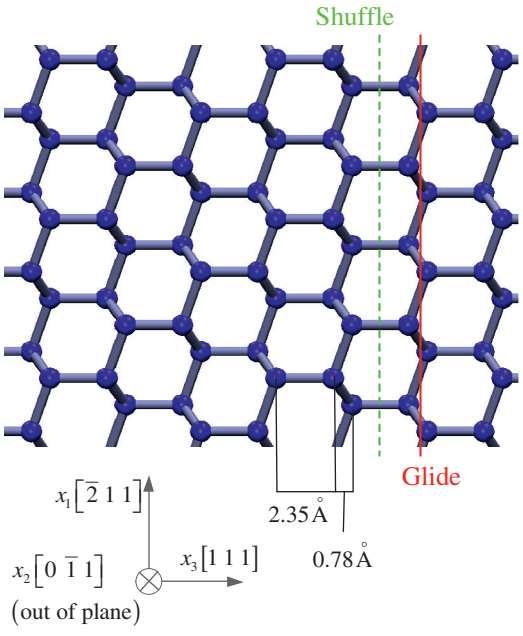

Fig. 2. Schematic representation of the crystal in the {1 1 0} projection showing the glide and shuffle planes.

When shuffle and glide dislocations are treated separately, one may wonder which value of G should be used in the PN model (Eq. (1)). It can be shown that the global G should be used for this purpose in both planes. The modulus appears in the PN model via the interaction term (second term in Eq. (1)) representing the elastic repulsion between the fictitious infinitesimal dislocations of the model. More specifically, this is the modulus appearing in the expression of the stress produced by an edge dislocation in its own glide plane. It can be shown (e.g. using an atomistic model) that this stress is identical whether the dislocation core resides in the glide or the shuffle plane. This is due to the fact that the far field, which results from the solution of the displacement-imposed boundary value problem of the Volterra dislocation, is written in terms of the global modulus, G.

3. Results and discussion

We consider two shuffle dislocations – a perfect screw and a 60° dislocation. Dislocations located on the shuffle plane are not dissociated and are known to control plasticity at low temperatures. Since the study presented here is athermal, the shuffle dislocations are more relevant for the present discussion. For completeness, we also discuss two partial dislocations, of 90° and 30° type, residing in the glide set of planes.

Let us focus first on the GGS corresponding to the four cases presented in Fig. 1. The traces of these surfaces in the direction of the Burgers vector are presented in Fig. 3. The reference curve is that for Case 1 in Fig. 1, in both shuffle and glide cases. The unstable stacking fault energy (USFE) for the $\langle 1\,1\,0\rangle$ shuffle trace is 1.38 J/m^2, while that for the $\langle 1\,1\,2\rangle$ glide trace is 4.79 J/m^2, in excellent agreement with those reported in Ref. [19]. These values should be compared with the USFE resulting from ab initio simulations [20] which are 1.84 J/m^2 and 2.51 J/m^2, respectively.

The GGS corresponding to Case 2 is different from the reference Case 1 for both shuffle and glide planes. The value of the USFE is not significantly different, but the position of the maximum shifts when a resolved shear strain of type 2 is applied. For the shuffle plane, the USFE is 1.38 J/m^2 for 1% and 3% strains, identical to the reference value. The USFE for the glide plane is 4.79 and 4.77 J/m^2 at 1% and 3% strain, respectively. The shift of the peak position indicates that the effective modulus changes as ε increases in Case 2. As the peak shifts, the curvature of the γ-surface at small relative displacements across the glide plane (small strains) changes. The curvature is proportional to the shear modulus. From the atomistic model, at 3% strain the effective shear modulus of the shuffle plane G_s decreases from 36.2 GPa to 35.3 GPa. Likewise, the corresponding modulus for the glide plane, G_g, decreases from 117 GPa to 103 GPa. The effective modulus G decreases by 4.5% (to 41.6 GPa) at 3% strain and by 10.7% (to 39 GPa) at 5% strain. The bonding across the glide plane depends only on s and is essentially unaffected by the far field, while the modulus reduction is due primarily to the contribution of second-nearest neighbors interaction across the glide plane. This observation is central in understanding the mechanics controlling the Peierls stress.

When a shear stress with a non-zero component in the direction perpendicular to the Burgers vector is applied (Case 3), the γ-surface is essentially identical to that of the reference case. This is in agreement with the well-established result that only the stress resolved in the direction of the Burgers vector matters for dislocation motion.

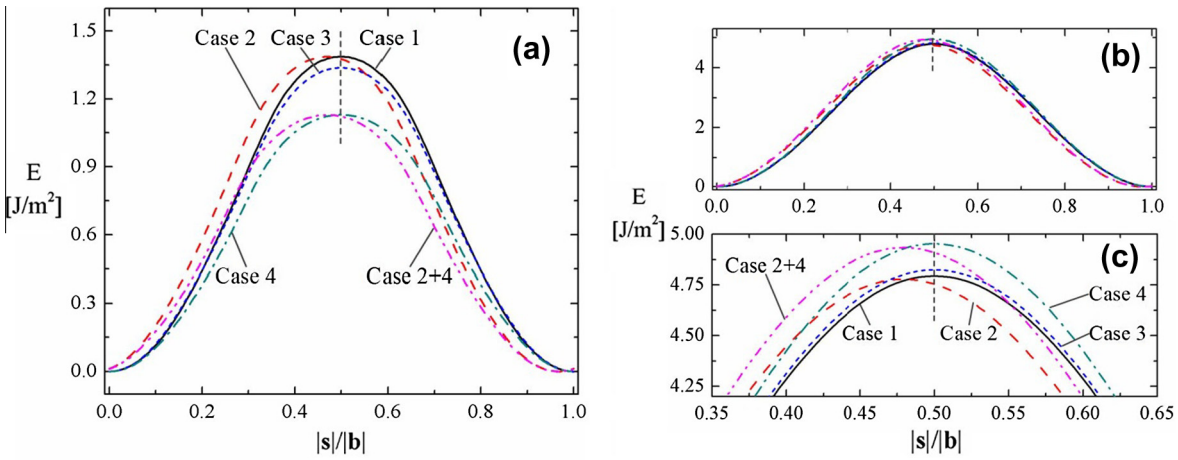

Fig. 3. γ-Surface traces in the ⟨1 1 0⟩ direction for the shuffle plane (a) and the ⟨1 1 2⟩ direction for the glide plane (b). A zoom-in of the glide set γ-surface trace close to the peak is shown in (c). The four curves correspond to Cases 1–4 shown in Fig. 1 and the combination of Cases 2 and 4. The dashed vertical lines indicate the position $|s|/|b| = 0.5$. For Cases 2 and 3, $|v| = 0.03$; for Case 4, $|v| = -0.03$.

Applying a compressive strain normal to the glide plane (Case 4) leads to different responses in the shuffle and glide planes. The USFE of the shuffle plane decreases significantly relative to the reference (1.3 and 1.13 J/m^2 at 1% and 3% compressive strain, ε_{33}, respectively), while that for the glide plane increases slightly (4.84 and 4.95 J/m^2 at 1% and 3% compressive strain, respectively). The maximum is located at $|s|/|b| = 0.5$ for all strains of type 4. This significant reduction of the USFE under compressive stress was also observed by Pizzagalli et al. [10] and appears to be a peculiarity associated with bonding in diamond cubic Si.

The superposition of the strains corresponding to Cases 2 and 4 does not lead to synergetic effects. The GGS changes as if the two effects add-up. For example, under a compressive normal strain of 3% combined with a shear strain of 3%, the USFE of the shuffle plane is 1.13 J/m^2 and is reached at $|s|/|b| = 0.53$. These values are equal to the USFE under pure compression with a 3% strain, and the value of the shift of the GGS maximum due to a 3% resolved shear strain in the direction of b. This superposition holds up to 10% strain in both shear and compression.

With these γ−surfaces one may evaluate the Peierls stress using the PN model. The results are shown in Fig. 4a and b for the shuffle and glide planes, respectively. The filled symbols correspond to Cases 1 (data points at zero normal strain) and 4 (other data points). The open symbols represent combinations of Cases 2 and 4. The Peierls stress decreases with increasing normal strain for the shuffle plane. This effect is due to the reduction of the USFE with the normal strain seen in Fig. 3a, Case 4. When the GGS is used (Case 2), the Peierls stress drops even more. This decrease is related to the reduction of the modulus, *G*. At strains corresponding to the Peierls stress (6–9 GPa range), the modulus, *G*, decreases by approximately 15–20% relative to the value of 43.6 GPa reported above. As observed in Fig. 4a, the Peierls stress for the screw dislocation is 20% smaller when the GGS is used, while the Peierls stress for the 60° dislocation is 13% smaller, both reductions being evaluated relative to Case 1. This clarifies the separate contributions of these two mechanisms to defining the value of the Peierls stress.

In other covalently bonded crystals with diamond cubic structure (diamond, SiC) one observes both increasing and decreasing trends for the Peierls stress with pressure [10].

These values should be compared with numerical data and experimental estimates available in the literature. Most of these are obtained for systems with zero normal strain (pressure). The Peierls stress computed directly from atomistic simulations using the same potential are indicated by the two arrows. The values are 5.8 GPa for the screw dislocation and 5.1 GPa for the 60° dislocation [4]. These are both below the PN estimates for Case 1 (8.8

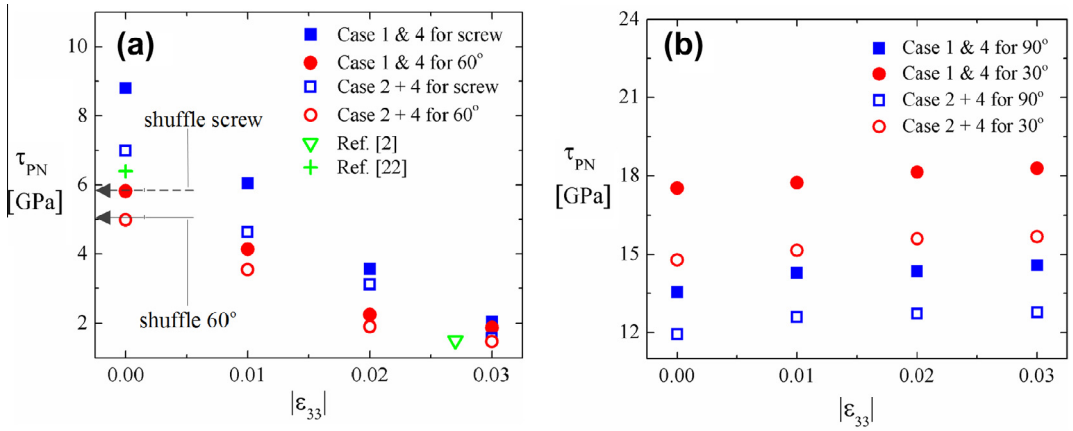

Fig. 4. Variation of the Peierls stress, τ_{PN}, with the absolute value of the compressive normal strain, $\varepsilon_{33} < 0$, (Case 4) for different in-plane shear values (Cases 1 and 1 + 4, filled symbols, and 2 and 2 + 4, open symbols) and for the shuffle (a) and glide (b) planes. The arrows in (a) indicate results from direct atomistic simulations. Available experimental data from Refs. [2,22] are also included for reference.

and 5.8 GPa, respectively) and hence the reduction introduced by the use of the GGS in Case 2 (to 6.9 GPa and 5 GPa, respectively) improves the agreement with the direct simulation data. Pizzagalli and Beauchamp [7] provide an estimate of 4.16 GPa for the Peierls stress of the shuffle screw dislocation based on first principle simulations. Furthermore, Wang [21] and Joos and Duesbery [5] use the formula estimating the Peierls stress in terms of the length of the Burgers vector and the interplanar separation, $\tau_{PN} = \frac{G}{1-\nu}(-4\pi d/|b|)$, and obtain 5.77 and 4.6 GPa for the shuffle screw and 60° perfect dislocations, respectively.

Experimental estimates of the critical stress are inherently indirect. These are obtained starting with the yield stress values measured at finite temperature, which are then extrapolated to 0 °K. Suzuki and Kojima [22] report 6.4 GPa for an unspecified dislocation type. A value for the Peierls stress for Si subjected to a pressure of 5 GPa is provided by Rabier et al. [2]. This pressure corresponds to a normal strain of 3.2% and the reported critical stress extrapolated to 0 °K is 1.5 GPa. This is in good agreement with the numerical data obtained here (Fig. 4a).

For completeness, the Peierls stresses for the two glide-set partials, 90° and 30°, are shown in Fig. 4b. The conclusions are similar to those discussed for the shuffle plane. The Peierls stress increases slightly with increasing compressive stress due to the slight increase of the USFE observed in Fig. 3b. Upon using the GGS, the estimate of the Peierls stress decreases substantially. This data supports the Peierls stress-controlling mechanisms discussed in conjunction with the shuffle plane.

4. Conclusions

Two ideas are discussed in this article. The first refers to the physical mechanisms controlling the Peierls stress. The critical stress is controlled mainly by the bonding across the glide plane, however, as the resolved applied shear stress increases, non-linear elasticity of the surrounding material lowers the instability threshold. The resolved shear stress does not modify the nature of bonding across the glide plane, leaving the USFE unchanged. The second advance is related to the use of the GGS in conjunction with the PN model for predicting the Peierls stress. We suggest that, from a physical point of view, this is more meaningful than the use of the regular γ-surface (Case 1).

Acknowledgments

This work was supported by IBM and the Center for Computational Nanotechnology Innovation (CCNI) at Rensselaer Polytechnic Institute.

References

[1] U.V. Waghmare, E. Kaxiras, M.S. Duesbery, Phys Stat. Sol. (b) 217 (2000) 545–564.
[2] J. Rabier, P.O. Renault, D. Eyidi, J.L. Demenet, J. Chen, H. Couvy, L. Wang, Phys. Stat. Sol. (c) 4 (2007) 3110–3114.
[3] J. Castaing, P. Veyssiere, L.P. Kubin, J. Rabier, Philos. Mag. A 44 (1981) 1407–1413.
[4] Q. Ren, B. Joos, M.S. Duesbery, Phys. Rev. B 52 (1995) 13223–13228.
[5] B. Joos, M.S. Duesbery, Phys. Rev. Lett. 78 (1997) 266–269.
[6] B. Joos, Q. Ren, M.S. Duesbery, Phys. Rev. B 50 (1994) 5890–5898.
[7] L. Pizzagalli, P. Beauchamp, Philos. Mag. Lett. 84 (2004) 729–736.
[8] H. Koizumi, Y. Kamimura, T. Suzuki, Philos. Mag. A 80 (2000) 609–620.
[9] E. Kaxiras, M.S. Duesbery, Phys. Rev. Lett. 70 (1993) 3752–3756.
[10] L. Pizzagalli, J.L. Demenet, J. Rabier, Phys. Rev. B 79 (2009) 045203 (1–7).
[11] V.V. Bulatov, S. Yip, A.S. Argon, Philos. Mag. 72 (1995) 453–496.
[12] F.R.N. Nabarro, Proc. Phys. Soc. 59 (1946) 23.
[13] S. Aubry, K. Kang, S. Ryu, W. Cai, Scripta Mat. 64 (2011) 1043–1046.
[14] F.H. Stillinger, T.A. Weber, Phys. Rev. B 15 (1985) 5262–5266.
[15] J. Tersoff, Phys. Rev. B 37 (1988) 6991–7000.
[16] J. Tersoff, Phys. Rev. B 38 (1988) 9902–9905.
[17] M.Z. Bazant, E. Kaxiras, J.F. Justo, Phys. Rev. B 56 (1997) 8542–8552.
[18] J. Godet, L. Pizzagalli, S. Brochard, P. Beauchamp, J. Phys.: Condens. Matter 15 (2003) 6943–6953.
[19] J. Godet, L. Pizzagalli, S. Brochard, P. Beauchamp, J. Phys.: Condens. Matter 15 (2003) 6943–6953.
[20] Y.M. Juan, E. Kaxiras, Philos. Mag. A 74 (1996) 1367–1384.
[21] J.N. Wang, Mater. Sci. Eng. A 206 (1996) 259–269.
[22] T. Suzuki, H. Kojima, Acta Metall. 14 (1966) 913–921.